Available online at www.sciencedirect.com
ScienceDirect
Ceramics International 37 (2011) 2031–2035
CERAMICS INTERNATIONAL
www.elsevier.com/locate/ceramint

Short communication

Pressureless sintering of silicon carbide ceramics containing zirconium diboride

Yang Hui, Zhang Lingjie, Guo Xingzhong*, Zhu Xiaoyi, Fu Xiaojian

Department of Materials Science and Engineering, Zhejiang University, Hangzhou, 310027, China

Received 15 July 2010; received in revised form 8 November 2010; accepted 26 January 2011
Available online 29 March 2011

Abstract

SiC-5 wt.% ZrB_2 composite ceramics with 10 wt.% Al_2O_3 and Y_2O_3 as sintering aids were prepared by presureless liquid-phase sintering at temperature ranging from 1850 to 1950 °C. The effect of sintering temperature on phase composition, sintering behavior, microstructure and mechanical properties of SiC/ZrB_2 ceramic was investigated. Main phases of SiC/ZrB_2 composite ceramics are all 6H-SiC, 4H-SiC, ZrB_2 and YAG. The grain size, densification and mechanical properties of the composite ceramic all increase with the increase of sintering temperatures. The values of flexural strength, hardness and fracture toughness were 565.70 MPa, 19.94 GPa and 6.68 MPa $m^{1/2}$ at 1950 °C, respectively. The addition of ZrB_2 proves to enhance the properties of SiC ceramic by crack deflection and bridging.

Keywords: C. Mechanical properties; Ceramics; X-ray diffraction; Microstructure

1. Introduction

Silicon carbide is a useful structural material because of its high strength and oxidation resistance at elevated temperatures, superior hardness and stiffness, high thermal conductivity, low coefficient of thermal expansion, and resistance to wear and abrasion [1–5]. The liquid phase sintering of SiC ceramic usually needs oxides as the sintering additives to improve their sintering and fracture toughness. The sintering additives, however, will weaken some mechanical properties of SiC ceramic to some extent. Study on further enhancement of the strength and fracture toughness of silicon carbide ceramics has evoked particular interest [6].

Zirconium diboride (ZrB_2) is one of the materials known as ultrahigh-temperature ceramics. It crystallizes into a hexagonal crystal structure of the AlB_2 type, which results in strong covalent bonding between boron–boron and metal–boron atoms, while the close packed metal layers exhibit characteristics consistent with metallic bonding [7]. This gives ZrB_2 a series of excellent properties, such as high melting point, hardness, and chemical stability [8–11]. Because of this unusual combination of properties, ZrB_2 has been proposed for use in various high temperature structural applications. The oxidation and thermal shock resistance of ZrB_2 also make it a candidate for thermal protection systems on future hypersonic flight vehicles [7].

By adding ZrB_2 to SiC, the resultant SiC–ZrB_2 ceramics have better strength and fracture toughness than monolithic SiC. Nevertheless, temperature has an important effect on the formation and amount of liquid phase and densification of SiC–ZrB_2 ceramics, which will decide their properties. Accordingly, in this work pressureless sintering of SiC–ZrB_2 composite at different temperatures was investigated. The aim of the study was to understand the effects of ZrB_2 and temperature on the densification, mechanical properties and microstructural features of SiC–ZrB_2 ceramics.

2. Experimental

Commercially available SiC powder (0.5–1 μm, >98%, Shandong Qingzhou Micropowder Co., Ltd., China), Al_2O_3 (~1 μm, >99%, Shanghai Wusi Chemical Reagent Co., Ltd., China), Y_2O_3 (~130 nm, >99%, Yixing 3-scionce Ultra-fine Powder Co., Ltd., China) and ZrB_2 (~0.5 μm, >97%, Dandong Chemical Engineering Institute Co., Ltd.) were used as raw powders. The powder mixtures of SiC plus 5% ZrB_2 plus

* Corresponding author. Tel.: +86 571 87953313; fax: +86 57187953054.
E-mail address: gxzh_zju@163.com (X. Guo).

0272-8842/$36.00
doi:10.1016/j.ceramint.2011.01.048

10 wt.% Al_2O_3 and Y_2O_3 mixture with a molar ratio of Y:Al = 3:5 were ball-mixed for 4 h in a steel container using silicon carbide balls and water as the grinding media. Subsequently, the slurry was dried by aqueous spray drying technique [12] and then sieved through a 200-mesh. The as-sieved powders were uniaxially pressed at a pressure of 100 MPa for 10 s. Cold isostatic pressing with an applied pressure of 250 MPa for 300 s was subsequently conducted. Sintering was carried out in a graphite element furnace at temperature ranging from 1850 to 1950 °C in vacuum (below 1000 °C) or in an argon atmosphere (above 1000 °C) for 15 min, and then at 1850 °C for 1 h. The sintered specimens were finished by machining before testing.

The final density was measured by the Archimedes method, while the relative density and contractiveness were estimated by the rule mixture. The microstructural features were analyzed by scanning electron microscopy (SEM, FEI Sirion, Holland) along with energy dispersive spectroscopy (EDS, EDAX Inc.) for chemical analysis. Crystalline phases were identified by X-ray diffraction (XRD) using Cu Kα radiation. The scanning rate was 2°/min and the scanning angles ranged from 10° to 80° with a sampling width of 0.02°. Flexural strength was tested in three point bending on 3 mm × 4 mm × 36 mm bars, using a 30 mm span and a crosshead speed of 0.5 mm min^{-1}. The edges of all the specimens were chamfered to minimize the effect of stress concentration due to machining flaws. Hardness (Hv 1.0) was measured by Vickers' indentation with a 9.8 N load applied for 15 s on polished sections. Fracture toughness (K_{Ic}) was calculated by the length of the cracks originating from the edges of the indentation marks, using the equation described by Niilara et al. [13]:

$$K_{Ic} = 0.018 H_v \sqrt{a} \left(\frac{E}{H_V}\right)^{0.4} \times \left(\frac{c}{a} - 1\right)^{-0.5} \quad (1)$$

where K_{Ic} is the fracture toughness of the materials, H_V the Vickers hardness, E the Young's modulus (for silicon carbide a value of 400 GPa was assumed), c the crack length and a the half indentation diameter.

3. Results and discussion

3.1. Sintering properties

The XRD spectra of the SiC/ZrB_2 ceramics sintered at different sintering temperatures are shown in Fig. 1. The phase analysis indicates the predominant phases are 6H-SiC, 4H-SiC, YAG and ZrB_2. YAG phase is presumably attributed to the reaction of Al_2O_3 and Y_2O_3 during sintering. From Fig. 1, it is noted that the peaks of 6H-SiC, 4H-SiC and YAG are identical at different temperatures, which indicates that the elevated temperature does not provide enough conditions for ZrB_2 to react with Al_2O_3, Y_2O_3 or YAG to form new phases during the sintering process, and SiC and ZrB_2 can play a role in the composites, respectively.

The sintering properties (relative density and shrinkage) of the specimens at different temperatures are presented in Fig. 2. Both relative density and shrinkage increased with the increase

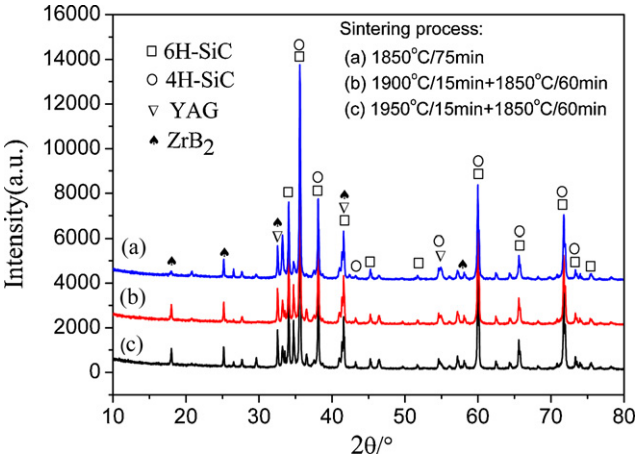

Fig. 1. XRD patterns of SiC/ZrB_2 composites ceramics at different temperatures.

of temperature. It is well-known that during pressureless sintering of silicon carbide with YAG as sintering aid, the reaction of Al_2O_3 and Y_2O_3 to form YAG phase takes place at the temperature higher than 1760 °C, and the formation and diffusion of the YAG phase accelerate with the increase of temperature, which thus promotes densification of the composites and results in the higher relative density and shrinkage. The sintering behavior of SiC/ZrB_2 shown in Fig. 2 confirms the argument above. In addition, the reduced porosity and grain coarsening also improved the relative density and shrinkage of the specimens.

3.2. Microstructure

Fig. 3 shows typical SEM photographs of fracture surfaces of the SiC/ZrB_2 composites. It was observed that the grain size of the samples was 0.5–2.5 μm, and increased with the increase of temperature. Compared with the size of SiC starting-powder (0.5–1 μm), there did not appear to be a rapid growth of SiC crystal, which indicated that ZrB_2 could restrain the growth of SiC crystals. It was also seen from Fig. 3 that the fractured mode of the composites was mainly intergranular fracture due to weak interface bonding and coupled with some transgranular

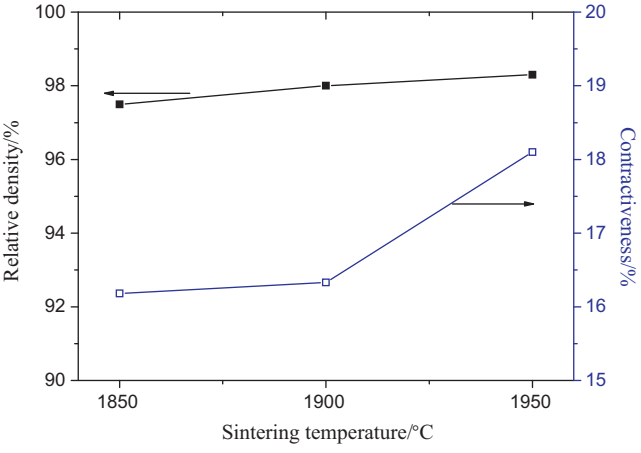

Fig. 2. Relationship between sintering properties and sintering temperatures.

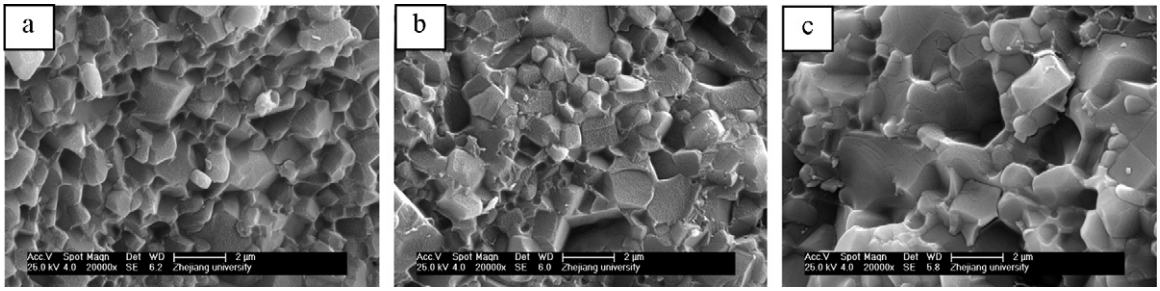

Fig. 3. SEM micrographs of fracture cross-sections of SiC/ZrB_2 composites at different temperatures: (a) 1850 °C/75 min; (b) 1900 °C/15 min + 1850 °C/60 min and (c) 1950 °C/15 min + 1850 °C/60 min.

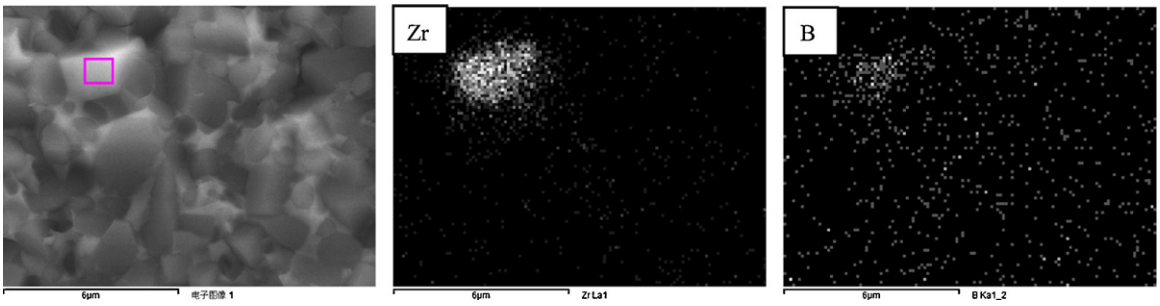

Fig. 4. Zr and B elements distribution of SiC/ZrB_2 composite ceramic sintered at 1950 °C/15 min + 1850 °C/60 min.

fracture. These surface pits in the SiC/ZrB_2 ceramic are indeed due to grain desquamation and not due to incomplete densification, which is evident from the high relative density of 98.3% [14].

The distribution of ZrB_2 in the composites is shown in Fig. 4. It can be observed that the white and rectangular ZrB_2 grains are uniformly distributed among the SiC grains. According to the previous research, YAG, which is insoluble in SiC, can segregate to the SiC interparticles zone [15], and the YAG grains enriched in the boundary of SiC grains in the SiC ceramic with YAG as sintering additive [16]. Meanwhile, with the increase of temperature, YAG provided a higher diffusivity transport path for Zr and B atoms and consequently make the interparticles zone including YAG and ZrB2 much more compact. The existence of SiC grains, YAG grains and ZrB_2 grains in grain boundary was beneficial to the bending strength, hardness and fracture toughness of silicon carbide ceramic. Therefore, more transgranular fracture appears at elevated temperature (Fig. 3(c)).

3.3. Mechanical properties

The measured mechanical property values at different temperatures are shown in Fig. 5. The flexural strength, hardness and fracture toughness of the specimens all increased with the increase of temperature, and the values were 565.70 MPa, 19.94 GPa and 6.68 MPa $m^{1/2}$ at 1950 °C, respectively. The improvement in flexural strength and toughness could be attributed to the densification of composites and the stronger interface bonding which is consistent with microstructure. The literature has reported that the hardness of a material with the addition of weak phases, such as carbon and flaws in the form of the pores and microcracks generally decreased [17], Accordingly, the increase in hardness was due

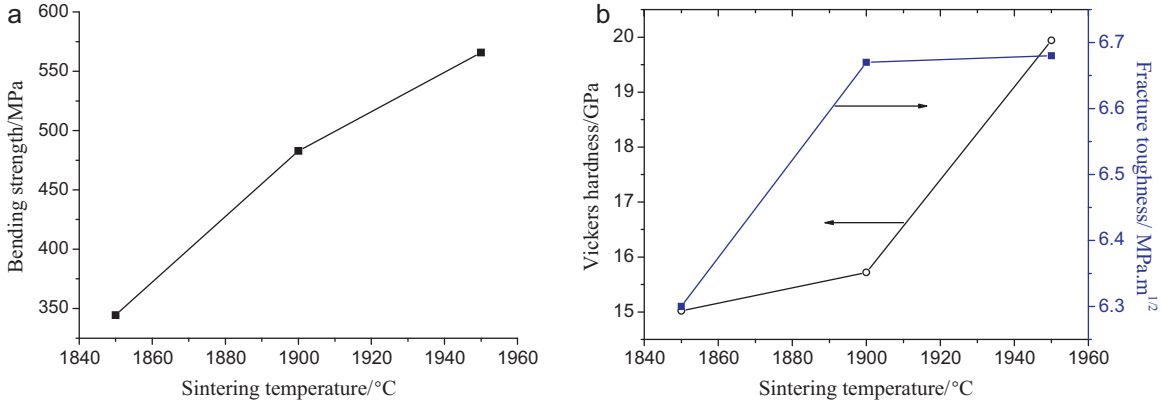

Fig. 5. Bending strength (a), hardness and fracture toughness (b) as a function of sintering temperature.

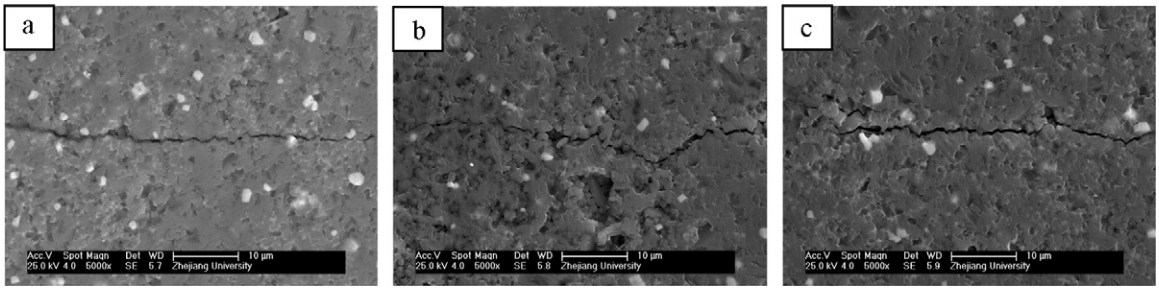

Fig. 6. SEM micrographs of polished cross-sections of specimens at different sintering temperatures: (a) 1850 °C/75 min; (b) 1900 °C/15 min + 1850 °C/60 min and (c) 1900 °C/15 min + 1850 °C/60 min.

to the reduction of pores in this work. All of these values are higher than those of SiC ceramic without ZrB_2 [16], indicating that ZrB_2 improved the mechanical properties of SiC ceramic.

3.4. Reinforcing mechanism

The above results have shown that the microstructure and properties of silicon carbide ceramic were improved by adding 5 wt.% ZrB_2. And the strengthening and toughening mechanisms of silicon carbide ceramics reinforced by ZrB_2 are analyzed as follows:

(1) *Crack deflection*. The SEM images of polished cross-sections with indentation crack paths for the specimens are shown in Fig. 6. In most cases, crack deflection occurred near the interfaces of SiC/ZrB_2 as well as SiC/SiC. The indentation crack path appeared most tortuous in the three samples. The more tortuous crack path can qualitatively indicate that more energy was absorbed and the crack driving force was more seriously consumed during crack propagation, thus leading to the materials toughening [18]. Compared to the sample at 1950 °C, fracture toughness of the one at 1850 °C was only 6.30 MPa $m^{1/2}$. The main reasons could be lower relative density and possibility of crack deflection declined. As the crack in sintered body at 1850 °C (Fig. 6(a)) appeared relatively straight with little deflection, which was consistent with declined fracture toughness.

(2) *Crack bridging*. In Fig. 7(b), it can be seen that the intergranular fracture accompanies with the transgranular one. When the main-crack met SiC crystal, it directly traversed the crystal to form transgranular fracture, due to high stress intensity of the crack. However, the main-crack branched off when it deflected to the grain boundary between ZrB_2 and SiC crystal to form intergranular fracture, which indicated that the crack bridge produced a force closure for two crack surfaces, which restrain the expansion of crack to enhance toughness fracture of silicon carbide ceramic. This was consistent with the theoretical model of crack bridging (Fig. 8).

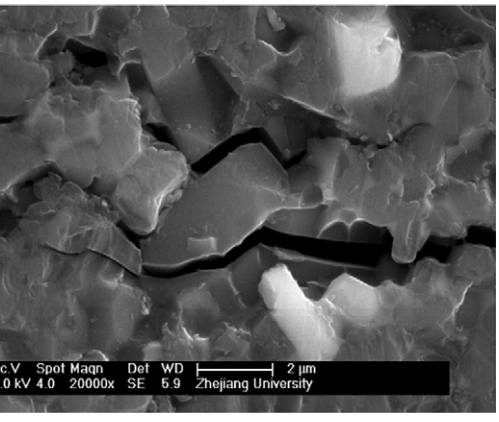

Fig. 7. Crack bridging of SiC/ZrB_2 composite ceramics.

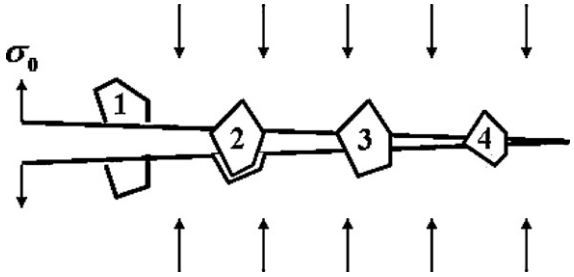

Fig. 8. Crack bridging mechanism.

4. Conclusions

SiC-5 wt.% ZrB_2 ceramics with 10 wt.% Al_2O_3 and Y_2O_3 as sintering aids were prepared by presureless sintering at temperature ranging from 1850 to 1950 °C. The addition of ZrB_2 improved the mechanical properties of SiC ceramic due to its segregation at triple points combined with YAG, while the elevated temperature promoted the densification of the SiC/ZrB_2 composite due to higher diffusivity transport path for all the atoms. This study clearly showed the addition of ZrB_2 into SiC is a promising way to improve the mechanical properties of SiC-based ceramics. The main phases of SiC/ZrB_2 composite ceramic are all 6H-SiC, 4H-SiC, YAG and ZrB_2 at different temperatures. The values of flexural strength, hardness and fracture toughness were 565.70 MPa, 19.94 GPa and 6.68 MPa $m^{1/2}$ at 1950 °C, respectively. The observed toughening mechanisms were crack deflection and bridging.

Acknowledgements

This work is supported by the Research Fund for the Doctoral Program of Higher Education (20070335017), the

High Science & Technique Key Project of Ministry of Education of China and the High Science & Technique Brainstorm Project of Zhejiang Province of China (no. 2006C11184).

References

[1] M. Singh, J.A. Salem, J. Eur. Ceram. Soc. 22 (2002) 2709–2717.
[2] J.E. Mark, P.D. Calvert, Mater. Sci. Eng. C1 (1994) 159–173.
[3] E. Vogli, H. Sieber, P. Greil, J. Eur. Ceram. Soc. 22 (2002) 2663–2668.
[4] P. Greil, T. Lifka, A. Kaindl, J. Eur. Ceram. Soc. 18 (1998) 1975–1983.
[5] P. Greil, J. Eur. Ceram. Soc. 21 (2001) 105–118.
[6] Xingzhong Guo, Hui Yang, Lingjie Zhang, Xiaoyi Zhu, J. Ceram. Int. 36 (2010) 161–165.
[7] A.L. Chamberlain, W.G Fahrenholtz, H.E. Gregory, J. Eur. Ceram. Soc. 29 (2009) 3401–3408.
[8] S.R. Levinea, E.J. Opilab, M.C. Halbigc, J.D. Kisera, M. Singh, J.A. Salema, J. Eur. Ceram. Soc. 22 (2002) 2757–2767.
[9] W.G. Fahrenholtz, G.E. Hilmas, I.G. Talmy, J.A. Zaykoski, J. Am. Ceram. Soc. 90 (5) (2007) 1347–1364.
[10] A.L. Chamberlain, W.G. Fahrenholtz, G.E. Hilmas, J. Am. Ceram. Soc. 89 (2) (2006) 450–455.
[11] D. Sciti, F. Monteverde, S. Guicciardi, G. Pezzotti, A. Bellosi, Mater. Sci. Eng. A 434 (2006) 303–312.
[12] X.Z. Guo, H.M. Li, X.Y. Zhu, H. Yang, J. Inorg. Mater. 23 (6) (2008) 1211 (in Chinese).
[13] K. Niihara, R. Morena, D.P.H. Hasselman, J. Mater. Sci. Lett. 1 (1982) 13.
[14] M. Singh, R. Asthana, Mater. Sci. Eng. A 460–461 (2007) 153.
[15] R.M. German, Z.A. Munir, Metall. Mater. Trans. A 7 (1976) 1873–1877.
[16] X.Z. Guo, H. Yang, J. Zhejiang Univ. Sci. 6B (3) (2005) 213.
[17] X.J. Zhou, G.J. Zhang, Y.G. Li, Y.M. Kan, P.L. Wang, Mater. Lett. 61 (2007) 960.
[18] G. Anne, S. Put, K. Vanmeensel, D. Jiang, J. Vleugels, O.V. Biest, J. Eur. Ceram. Soc. 25 (2005) 55–63.